

A Computational Study of 3-D Helium Clusters

Hassan Sabzyan* and Farzaneh Zanjanchi[#]

Department of Chemistry, University of Isfahan, Isfahan, 81746-73441, I. R. Iran

Physical and thermodynamic properties have been calculated and analyzed for the best and optimized geometries of the 3-D clusters with $N = 3$ to $N = 10$ atoms and unit cells of three types of crystalline systems using *ab initio* RHF/6-31G** method. Dependence of the lattice binding energy on the cluster parameter, R , has been studied. Similar behavior observed for the binding energies for all clusters shows that probabilities of their existence in the condensed phase are more or less the same. In the next step, thermodynamic properties have been calculated and analyzed for He_{27} 3-D helium clusters with simple cubic, body centered cubic (bcc), trigonal and hexagonal (hcp) configurations. The results show that the hexagonal cluster is more favored over other clusters. It is found that these clusters are electronically stable over a limited range of the values for the lattice parameter. $\Delta_f H$ is constant in this stability region and thus the $\Delta_f G$ exactly follows the variations of $T\Delta_f S$. Surface effects have been investigated by comparing the square and hexagonal He_9 2-D lattices with the cubic and hexagonal He_{27} 3-D lattices, respectively. The lattice parameters, densities and molar volumes calculated for the clusters with hcp and bcc configurations have satisfactory agreement with the available experimental values. Properties of the He_{13} , He_{34} and He_{104} hcp clusters have also been calculated and analyzed.

Keywords: Helium; Cluster; 3-D; *Ab initio*; hcp; bcc; Density.

INTRODUCTION

The structure and dynamics of clusters of different sizes, i.e. of aggregates of identical partners bound by either chemical forces or by weaker physical interactions, usually show a set of different properties from either the atomic components or the corresponding mesoscopic bulk structures.¹ We can consider small atomic and molecular clusters as nano systems showing a variety of properties different from those of both the isolated atoms and molecules and the corresponding bulk system which can be employed for specific new applications, e.g in nanoscale devices. At the same time, these clusters can be studied using standard theoretical and computational methods used at the molecular level to interpret and understand their behavior.^{2,3} Clusters of rare gases (Rg) formed by weak van der Waals (vdW) interactions, and their capacity to act as inert solvents for atomic and molecular dopants^{4,5} have received a great deal of attention in the past two decades and have provided a very useful ground for applying and evaluating the ability of computational and theoretical (both quantum and classical) methods to accurately interpret a broad variety of observed properties.⁶⁻⁹

Inert gases in many aspects form the simplest structure of the condensed phase. Chemists have not yet been able to synthesize macroscopic quantities of chemical compounds containing helium, neon, and argon. Clusters and molecules containing atoms of these gases are stable for short periods of time and detectable only in solid matrices at very low temperatures. Therefore, it is usually stated that the threshold of actual chemical reactivity is reached at krypton,¹⁰ and the lightest noble gases are still perceived as essentially inert. In less usual environments, as compared to the traditional chemistry laboratories such as the low-pressure or high-pressure gaseous phase or the low-temperature solid matrices, however, one discovers a large number of stable or metastable species containing helium, neon, and argon, questioning validity of the chemical inertness of these elements. The observed neutral molecules and ions containing inert gas atoms range from simple small-size molecular fragments or complexes to large-size encapsulation products with the noble gases included in a cage. Computational techniques, usually employed to elucidate the structure, bonding, and properties of the experimentally observed species, are also used to reveal yet unknown rare gas compounds and to suggest conceivable routes to their

* Corresponding author. E-mail: sabzyan@sci.ui.ac.ir

[#] Present address: Azad Islamic University of Takestan, Takestan, 34815-315, I. R. Iran.

preparation.¹¹⁻¹³

The chemistry of gaseous and solid phase species containing helium, neon, and argon is indeed a fascinating interplay between theory and experiment, and the relevant covered literature is already impressively large.¹⁴⁻¹⁹ Helium is in principle the most inert monoatomic gas. It has the highest ionization potential (24.587 eV) and the lowest polarizability (0.205 \AA^3)²⁰⁻²¹ of all chemical elements and therefore appears as a very hard sphere, extremely difficult to bind. The necessary quantum correction for the kinetic energy is larger for a helium atom than that for other inert gases.²²

The binding energy of an inert gas crystal is simply obtained by adding the potential energy of all atoms of the crystal. For an N -atom crystal of inert gas, the per-atom total potential energy, assuming a Lennard-Jones potential,²³ is given by

$$U_{\text{tot}} = \frac{1}{2} N(4\varepsilon) \left[\sum_j \left(\frac{\sigma}{\rho_{ij}R} \right)^{12} - \sum_j \left(\frac{\sigma}{\rho_{ij}R} \right)^6 \right] \quad (1)$$

where $\rho_{ij}R$ is the distance between each atom j and the reference atom i expressed in terms of the shortest distance between the nearest neighbors, R . The factor $\frac{1}{2}$ takes care of the overcounted interactions. In Eq. (1), σ , the hard sphere collision diameter, is the distance corresponding to the zero energy of the i - j inter-atomic interaction potential. Summation Σ in Eq. (1) converges quickly for body centered cubic (bcc) and hexagonal (hcp) structures. Therefore, only the first few nearest neighbors contribute mainly to the total interaction energy of the crystals of inert gases. The interaction energy, ε , depends on the type of the interacting species of the lattice. Calculations based on Eq. (1) predict that the bcc structure is preferred by Xe, Kr and Ar, while He prefers an hcp structure.²³⁻²⁴

Prediction of the boiling point of liquid helium and its PVT behavior using *ab initio* methods is the ultimate aim of this series of studies. In the first part of our studies, we examined ability of the RHF/6-31G** method in predicting comparative properties and behaviors of the 1-D and 2-D helium lattices.²⁴ It was discussed there that although the RHF method may not be able to predict exact numerical values of the physical quantities of systems with weakly interacting particles, its comparative predictions are valid enough for qualitative analysis of the behavior of these system.

Here, in this work we have extended our studies to the small 3-D clusters of He atoms. In the following sections,

first, computational procedures used in this work will be presented. Next, the characteristics obtained for helium clusters with different configurations will be presented and discussed. Then, helium clusters with unit cells of three crystal-systems in eight different crystal lattices are studied. Finally, characteristics of the He₂₇ 3-D helium clusters with simple cubic, body centered cubic, trigonal and hexagonal configurations are calculated and compared with those of the square and hexagonal He₉ 2-D lattices and with available experimental data.

COMPUTATIONS

In 3-D space, point symmetric groups allow seven types of crystalline systems and fourteen types of various crystalline lattices among which only the three systems cubic (cubic P or simple cubic, cubic I or bcc, cubic F or fcc), tetragonal (tetragonal P and tetragonal I) and orthorhombic (orthorhombic P, orthorhombic C and orthorhombic I) crystal lattice types have been considered in this study. In the optimization procedures of different 3-D He clusters, geometrical constraints of the unit cells corresponding to these crystal lattices have been imposed. Potential energy surfaces of the breathing mode of vibration are derived for the unit cell clusters by varying the lattice parameter. For the calculation of thermochemical properties, vibrational analyses were carried out within the same level of theory and with the same basis set used for the geometry optimization with a scale factor of 0.8929. The imaginary frequencies found for some of the clusters show that these clusters are not quantum mechanically stable within the imposed geometries. It is practically impossible or very difficult to locate the absolute minimum point on the potential hypersurface of the large clusters with all inter-atomic distances and bond angles released, but this is possible for small clusters; the best geometries obtained for clusters with three and four atoms, for example, are equilateral triangle and regular tetragonal, respectively. All calculations have been carried out using the RHF/6-31G** method with G94 and G98 software.²⁵

RESULTS AND DISCUSSION

3-D helium clusters

The calculated values of the per-atom binding ener-

gies defined as $E_b = -\Delta E = -[E(\text{He}_N) - N E(\text{He})]/N$ and the optimum geometric parameters are reported in Table 1. From the results presented in this Table, it can be seen that values of binding energy and optimized lattice parameter do not have well defined dependence on the number of atoms of the cluster. Positive binding energy and zero number of negative modes obtained for most clusters in these calculations correspond to the quantum stability of these helium clusters. Negative modes obtained for some of the clusters may be attributed to the constrained bond lengths and angles of the non-suitable imposed geometry of these clusters.











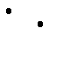
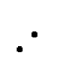
Dependence of the lattice binding energy on the lattice parameter over the range of $R = 3.0\text{-}4.0 \text{ \AA}$ for different clusters containing 3-10 atoms is shown in Fig. 1. This R -dependence of the binding energy can be regarded as the potential energy curve of the breathing mode of vibration of the lattice. Fig. 1 shows that minima of the binding energy curves for all clusters occurring around $R = 3.2 \text{ \AA}$. The R -dependences of the obtained potential energies are similar to typical anharmonic diatomic vibration potential.

These results show that all of these clusters may exist in the liquid and polycrystalline solid phases. Similar behavior observed for the binding energies for all clusters show that their existences in the condensed phase are more or less equally probable.

The calculated values of the depths and widths of the potential wells of the breathing modes of vibration depend on the configuration type and are almost independent of the number of helium atoms of the cluster. Except for the simple cubic lattice, all of the examined lattices have complex geometries with a variety of He-He distances (bond lengths). In a thermalized liquid and in a polycrystalline solid, all of possible clusters with different lattice types may exist, however with different statistical weights or probabilities. This makes the *ab initio* theoretical study of He in the condensed phases even more difficult. Due to their different electronic spatial extents, $\langle R^2 \rangle$, probability of the existence of different clusters with the same number of He atoms but with different geometries vary with pressure, temperature and density.

The results obtained for the unit cell 3-D clusters re-

Table 1. Number of negative modes N_{im} , optimized lattice parameter R (in \AA), electronic spatial extent $\langle R^2 \rangle$ (in au), and per atom binding energy E_b (in cm^{-1}), heat capacity C_V/N and entropy S/N (both in $J/molK$), calculated for different 3-D helium clusters using RHF/6-31G** method

Cluster						
	He ₃	He ₄	He ₅	He ₆ -(a)	He ₆ -(b)	He ₇ -(a)
N_{im}	0	0	0	0	3	2
R	3.18987	3.19216	3.18775	3.14330	3.18916	3.19215
$\langle R^2 \rangle$	79.6	118.4	301.9	233.0	268.2	452.9
E_b	0.358	0.527	0.289	0.687	0.530	0.599
C_V/N	16.6	18.7	20.0	20.8	16.6	19.0
S/N	102.2	105.0	159.2	106.2	86.0	101.3
Cluster						
	He ₇ -(b)	He ₈	He ₉ -(a)	He ₉ -(b)	He ₉ -(c)	He ₁₀
N_{im}	9	6	3	8	11	11
R	3.18753	3.18351	3.19388	3.19037	3.14309	3.18768
$\langle R^2 \rangle$	451.7	452.9	603.8	602.5	585.4	758.3
E_b	0.307	0.535	0.619	0.549	0.412	0.463
C_V/N	10.7	15.6	19.4	14.8	12.0	13.3
S/N	60.5	75.4	98.6	74.8	67.5	65.9

ported in Table 2 show that the unit cells which have no negative modes have larger binding energies as compared to the other types of unit cells. No correlation is found between the calculated binding energy and the point group symmetry and the number of atoms of the lattice unit cell. The largest binding energy is obtained for the unit cell of the orthorhombic lattice C (O-C) in which the two helium atoms located in the two parallel faces have the shortest distance. Also, the binding energy for the packed lattice obtained is $0.488 \text{ cm}^{-1}/\text{atom}$ which is less than that obtained for the rectangular lattice with the optimized unit cell dimensions $R_1 = 3.2$, $R_2 = 3.9$ and $R_3 = 3.9 \text{ \AA}$.

Thermodynamic analysis of different He_{27} 3-D clusters

Thermodynamic stability of the He_{27} 3-D clusters in four types of lattices (simple cubic, body centered cubic, trigonal with 60° angle and hexagonal unit cells) have been analyzed based on their formation Gibbs free energies $\Delta_f G$. The geometries of these He_{27} 3-D clusters are plotted in Fig. 2. The results of this study are demonstrated in Fig. 3. This figure shows that formation of this cluster in different lattices is electronically possible only at certain ranges of the lattice parameter values.

In order to locate the stability range of each cluster,

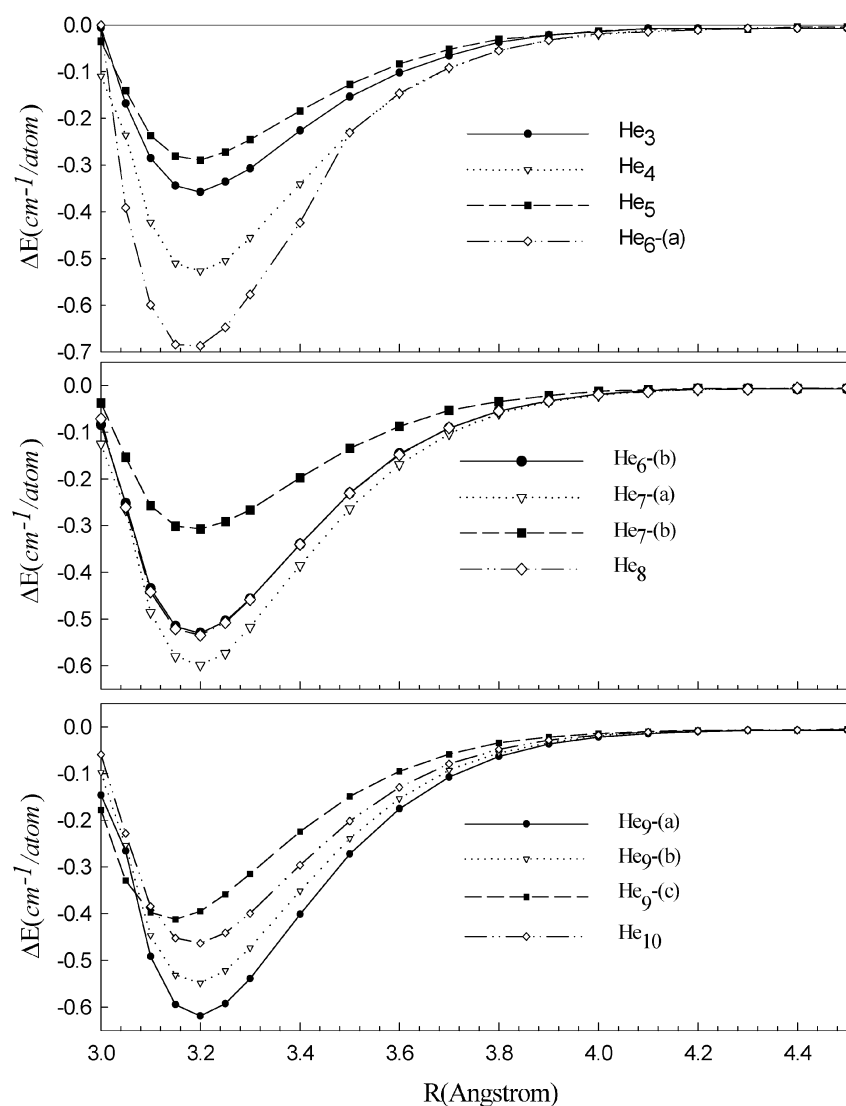
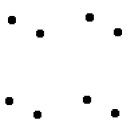
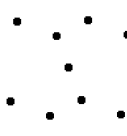
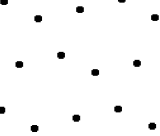
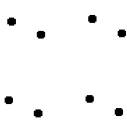
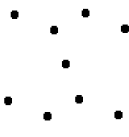
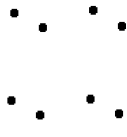
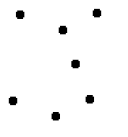



Fig. 1. Dependence of the per atom binding energy, $\Delta E \text{ (cm}^{-1}/\text{atom)}$, on the lattice parameter R (i.e. the potential energy curve for the breathing mode of vibration of the lattice) calculated for different 3-D helium clusters containing 3 to 10 atoms (Table 1) using the RHF/6-31G** method.

Table 2. Number of negative modes N_{im} , optimized lattice parameters R_i (in Å), electronic spatial extent $\langle R^2 \rangle$ (in au), and per atom binding energy E_b (in cm^{-1}), heat capacity C_V/N and entropy S/N (both in $J/molK$), calculated for different 3-D helium clusters with unit cells of three crystal-systems in eight different crystal lattices using RHF/6-31G** method

Cluster				
	He ₈	He ₉	He ₁₄	He ₈
Lattice	Simple Cubic	Cubic I (bcc)	Cubic F (fcc)	Tetragonal P
Point Group	O _h	O _h	O _h	D _{4h}
Calculation	Z-Matrix	Both	Cartesian	Cartesian
N_{im}	0	11	0	0
E_b	0.535	0.407	0.884	0.510
R_1, R_2, R_3	3.2, 3.2, 3.2	3.6, 3.6, 3.6	4.5, 4.5, 4.5	3.2, 3.2, 3.3
$\langle R^2 \rangle$	457.4	576.3	1117.3	466.7
C_V/N	21.8	12.0	23.2	21.8
S/N	116.4	75.9	101.3	115.6
Cluster				
	He ₉	He ₈	He ₉	He ₁₀
Lattice	Tetragonal I	Orthorhombic P	Orthorhombic I	Orthorhombic C
Point Group	D _{4h}	D _{2h}	D _{2h}	D _{2h}
Calculation	Both	Cartesian	Cartesian	Cartesian
N_{im}	1	4	1	0
E_b	0.624	0.444	0.605	0.582
R_1, R_2, R_3	3.2, 3.2, 4.5	3.1, 3.2, 3.3	3.2, 3.3, 4.4	3.2, 3.3, 5.5
$\langle R^2 \rangle$	606.0	485.6	599.9	793.7
C_V/N	21.2	17.7	21.2	22.4
S/N	110.4	101.0	109.4	116.9

the number of negative modes is calculated and followed with changing lattice parameter. As can be seen from Table 3, three of these lattices are electronically stable only over a limited range of the lattice parameter values, and the fourth lattice does not show any stability range without negative modes. These ranges for the cubic and trigonal lattices are identical. Analysis of the geometries of these He₂₇ 3-D clusters plotted in Fig. 2 show that hexagonal and body centered cubic clusters studied here do not form a complete multiple of the corresponding unit cells in an organized way as occur in the actual macroscopic lattice. Although the constrained geometry of having single values for the nearest neighbors He-He distance is not realistic, the results can well serve the purpose of the present work for the

comparative study of the $\Delta_f G$ values of different 3-D helium clusters.

Variations of the $\Delta_f G$ values for the He₂₇ clusters with simple cubic and trigonal configurations are similar. In the stability region, where the cluster has no imaginary frequency, the $\Delta_f G$ values for the trigonal cluster are lower than those for the simple cubic cluster. In our previous work on the 2-D He lattices,²⁴ the same trend is observed for the corresponding 2-D lattices (we can assume that the 3-D clusters are formed by stacking three layers of the corresponding 3 × 3 2-D He lattices. Comparison between the R- $\Delta_f G$ curves calculated for the corresponding 2-D and 3-D clusters are presented in Fig. 4. It can be seen from this Figure that the 2-D lattices are more stable than the corre-

Table 3. Number of negative modes, N_{im} , obtained for the He_{27} 3-D clusters over different ranges of the lattice parameter using the RHF/6-31G** method. The highlighted section shows the stability range in which $N_{\text{im}} = 0$. Characteristics of the minimum point of the $R-\Delta_f G$ curves, R_{min} (in Å) and $\Delta_f G_{\text{min}}$ (in kJ/mol), are also reported in the last two rows

Cubic		Trigonal		Hexagonal		Cubic-I	
R	N_{im}	R	N_{im}	R	N_{im}	R	N_{im}
3.00-3.17	21	3.00-3.17	12	3.00	2	3.00	20
3.18-3.19	7	3.18-3.19	11	3.10	1	3.10	24
3.20-3.36	0	3.20-3.36	0	3.25-3.37	0	3.20	26
3.37	12	3.37	9	3.37	1	3.30-3.50	25
3.38	52	3.38	30	3.38	2	3.60-3.70	24
3.39	54	3.39	44	3.39	62	3.80-4.00	60
R_{min}	$\Delta_f G_{\text{min}}$	R_{min}	$\Delta_f G_{\text{min}}$	R_{min}	$\Delta_f G_{\text{min}}$	R_{min}	$\Delta_f G_{\text{min}}$
3.36	-45.27	3.36	-28.10	3.369	-55.36	3.80	281.10

sponding 3-D lattices. The stability ranges for the two corresponding 2-D and 3-D clusters are more or less the same. In these ranges, the slope of the $R-\Delta_f G$ curves for the 3-D lattices are larger than those for the corresponding 2-D lattices. Fig. 4 shows also that the thermodynamic difference between the 2-D and 3-D lattices is smaller at the higher end of the stability region. Results also show that the difference between the two types of 3-D clusters is much larger than that of the corresponding 2-D lattice.

The calculated values of $\Delta_f G_{\text{min}}$ at the minimum of the stability range (reported in Table 3) for the hexagonal cluster are more negative than the corresponding values for the other three types of lattices. This, plus the zero number of negative modes, shows that a hexagonal cluster is quantum mechanically and thermodynamically stable. Therefore, it can be said that a hexagonal lattice is the most favored

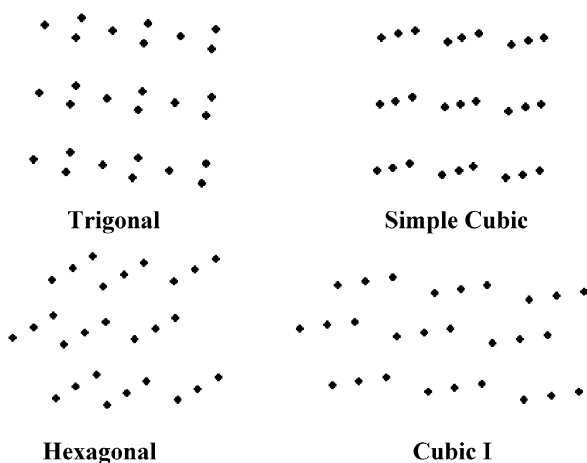


Fig. 2. The He_{27} 3-D clusters with different crystal lattices studied in this work.

structure for solid helium which is in perfect agreement with the experimental data.²⁶ It should however be mentioned that crystallization of the solid helium in the cubic and the trigonal lattices are also possible but with lower probability. In accordance with this prediction, the experimental results have shown also that in a helium solid sample, small amounts of bcc state exist for densities lower than 0.1932 gr/cm^3 , and the bcc structure composition increases with a decrease in density, so that at densities lower than 0.1906 gr/cm^3 , no solid helium sample can be found in a pure hcp state.²⁶ Based on these results only bcc and hcp clusters will be considered for further study in the rest of this report.

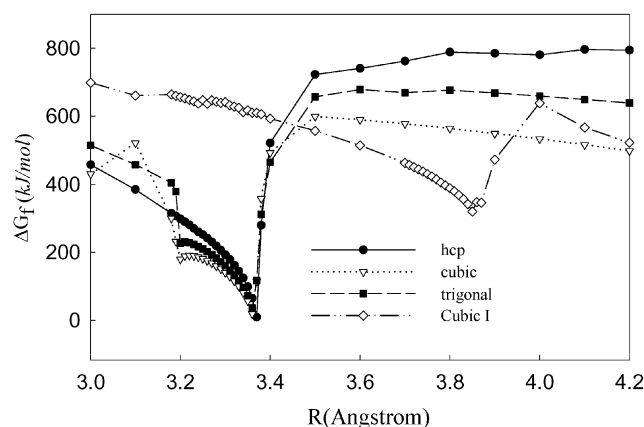


Fig. 3. Variation of the formation Gibbs free energy $\Delta_f G$ (298 K, 1 atm) in kJ/mol as a function of lattice parameter for He_{27} clusters in four types of configurations, hexagonal (hcp), simple cubic, trigonal and cubic I lattices calculated at the RHF/6-31G** level of theory.

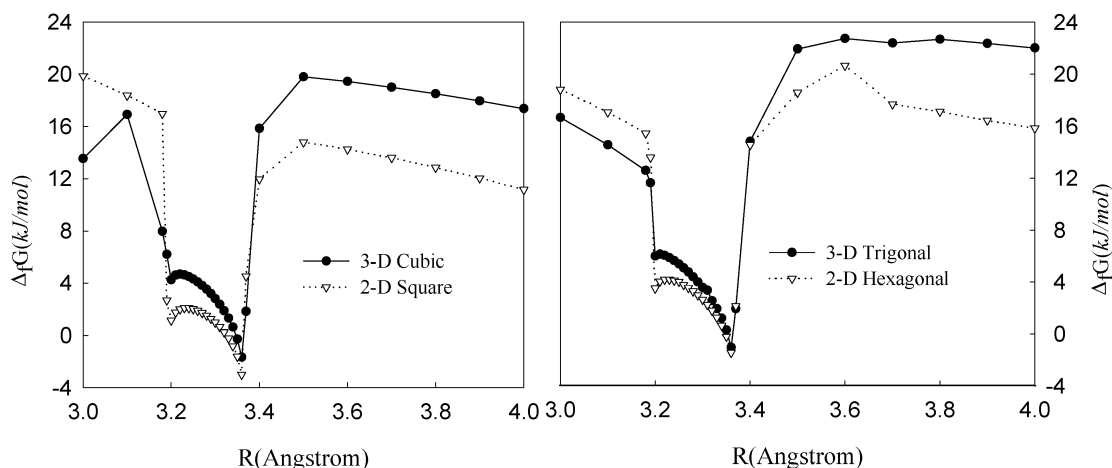


Fig. 4. Comparison of the R-dependences of the formation Gibbs free energies of the corresponding 2-D²⁴ and 3-D helium lattices obtained at RHF/6-31G** level of theory.

3-D helium clusters with hcp unit cells

Variations of $\Delta_f G/N$ for three hexagonal He_N clusters with $N = 13, 34$ and 104 (Fig. 5) have been plotted in Fig. 6 as a function of the lattice parameter. The He_{34} and He_{104} clusters are complete multiples of the hcp unit cells.

Fig. 6 shows that comparative trends of the functional forms of $\Delta_f G/N$ and its minimum value, $\Delta_f G_{\min}/N$, are almost the same for all clusters, but the values of the lattice parameter at the minimum point for the He_{104} cluster slightly differs from those of the other two clusters by 0.05 \AA . The difference between the results obtained for the He_{104} and the other two lattices is partly due to the use of a differ-

ent basis set. Calculations with the 6-31G** basis set on this lattice was not possible due to our limited hardware facilities. As a result of this study, the optimized value of the lattice parameter for the hcp cluster in its thermodynamically most stable state is found to be $R = 3.369 \text{ \AA}$. Based on this value, and by fitting a rectangular cube over 30 atoms of the hcp cluster, the approximate density and molar volume of a solid hexagonal helium sample with pure hcp structure are calculated as:

$$\rho = \frac{30 \text{ atom} \times 4.0026 \text{ gr/mol} / 6.02 \times 10^{23} \text{ atom/mol}}{[11.6706 \times 10.1070 \times 8.2523 \text{ \AA}^3]} \times \left(\frac{1 \text{ \AA}}{10^{-8} \text{ cm}} \right)^3 = 0.2049 \text{ gr/cm}^3 \quad (2)$$

$$\bar{V} = \frac{M}{\rho} = \frac{4.0026 \text{ gr/mol}}{0.2049 \text{ gr/cm}^3} = 19.5344 \text{ cm}^3/\text{mol} \quad (3)$$

The experimental values of the lattice parameter, density and molar volume are reported to be 3.655 \AA , 0.2 gr/cm^3 and $24.75 \text{ cm}^3/\text{mol}$ for ^4He and 3.561 \AA , and $20.75 \text{ cm}^3/\text{mol}$ for ^3He , respectively.^{26,27} A comparison between these experimental values and our computational results shows that the calculated values of lattice parameter, density and molar volume are reliable and acceptable within accuracy of the computational method used in this study and the typical experimental error bars.

The difference between molar volumes of the two helium isotopes which should ideally be identical is due to the

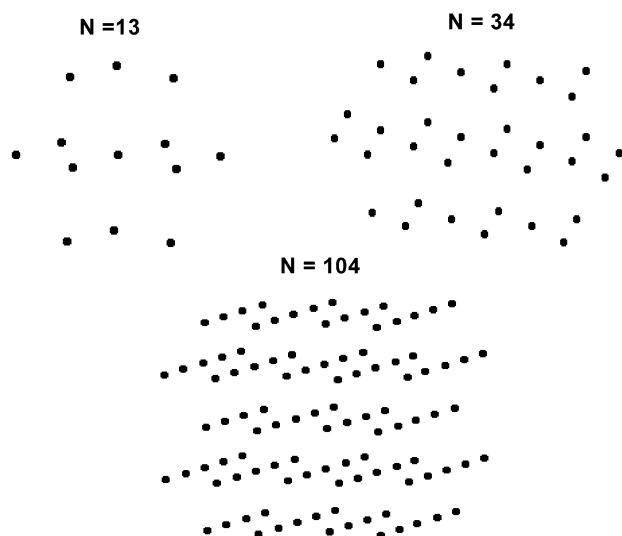


Fig. 5. Different He_N clusters with hcp configuration studied in this work.

difference in quantum nuclear statistics of the two isotopes. Since present computations are carried out at the HF level of theory, this difference cannot be distinguished by the results obtained in this work.

Variations of $\Delta_f H$ and $\Delta_f S$ values (at 1 atm and 298.15 K) with the lattice parameter for the He_{13} hcp cluster have been plotted in Fig. 7. This Figure shows that $\Delta_f H$ value is constant in the stability region and thus variation of $T\Delta_f S$ is exactly (with a minus sign) followed by $\Delta_f G$ in this region. Therefore, as found for the 2-D lattices, at 1 atm and 298.15 K trend of the $\Delta_f G$ variations are only due to the variations of $T\Delta_f S$ values.

3-D helium clusters with bcc unit cells

Variations of calculated values of $\Delta_f G/N$ (at 1 atm and

298.15 K) for the He_9 (a unit cell), and He_{30} clusters with bcc configuration (Fig. 8) with the lattice parameter are plotted in Fig. 9. This Figure shows that functional forms of $\Delta_f G/N$ for the two clusters have few similarities. The $\Delta_f G/N$ value for the bcc unit cell (He_9) decreases considerably in two regions each having two distinctly separated minima. A similar but weaker behavior with only one minimum in each region is observed for the larger He_{30} bcc cluster. The difference between the two minimum values of $\Delta_f G_{min}/N$ for the He_{30} cluster is larger than that for the bcc unit cell, He_9 . The limited size of the clusters studied here may have a significant effect on the calculated properties (this is the well known surface effect studied already for the 2-D helium lattices²⁴). Therefore, the large difference between the results obtained for these two bcc clusters can be attributed

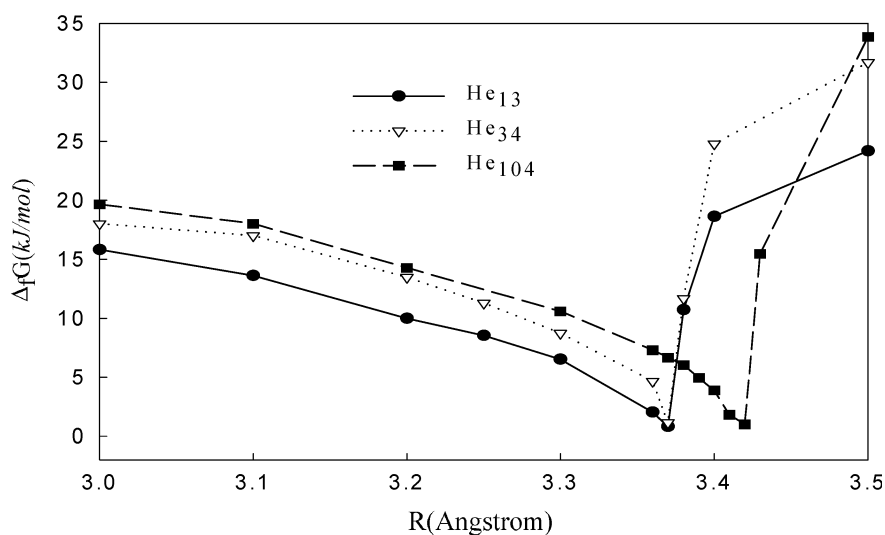


Fig. 6. Variations of $\Delta_f G/N$ with the lattice parameter for He_N clusters with hcp configurations obtained at 1 atm and 298.15 K using the RHF/6-31G** method for He_{13} and He_{34} and the RHF/6-31G method for He_{104} .

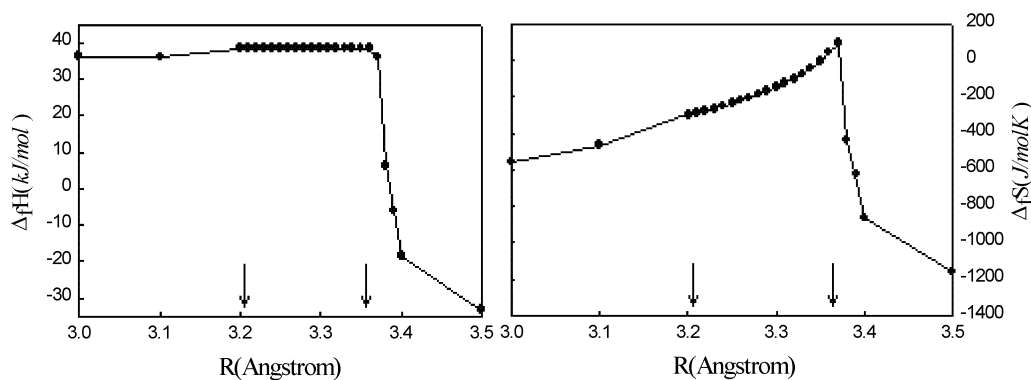


Fig. 7. Variations of $\Delta_f H$ and $\Delta_f S$ (298 K, 1 atm) with the lattice parameter for the He_{13} cluster with a hcp lattice calculated at the RHF/6-31G** level of theory. The arrows mark limits of the stability region.

to this surface effect. This effect is considerably decreased if sufficiently large clusters are used, and ideally vanishes if the calculated properties are extrapolated to the infinitely large clusters. Such an extrapolation would be possible for computational results if several large clusters could be studied.

Thermodynamic properties are calculated for the optimized structures of the bcc helium clusters on the basis of the minimum point of $\Delta_f G/N$ (at $R = 3.82 \text{ \AA}$) for the He_{30} cluster. Density of the solid bcc helium is thus calculated as:

$$\rho = \frac{30 \text{ atom} \times 4.0026 \text{ gr/mol} \times 6.02 \times 10^{23} \text{ atom/mol}}{[11.46 \times 13.28 \times 7.64 \text{ \AA}^3]} \times \left(\frac{1 \text{ \AA}}{10^{-8} \text{ cm}} \right)^3 = 0.1491 \text{ gr/cm}^3 \quad (4)$$

The calculated value of density for the bcc structure is significantly less than that obtained for the hcp. This is in per-

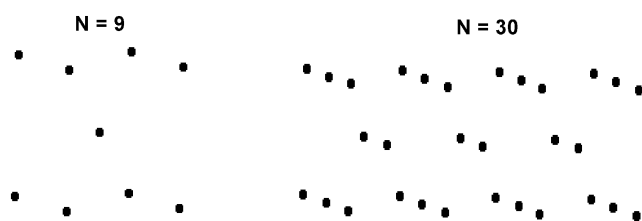


Fig. 8. Structures of the two He_9 and He_{30} helium clusters with bcc configuration studied at the RHF/6-31G** level of theory.

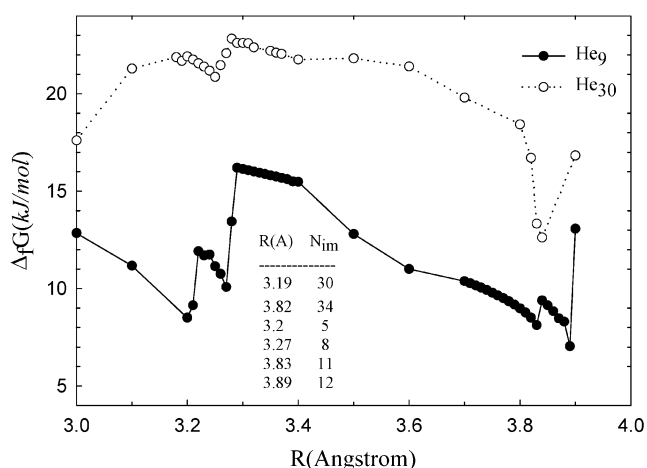


Fig. 9. Variations of $\Delta_f G/N$ at 1 atm and 298.15 K with the lattice parameter, R , for a unit cell, He_9 , and the He_{30} cluster with bcc configuration calculated with the RHF/6-31G** method.

fect agreement with the experimental results.²⁶⁻³⁰ Our computations however show that the bcc structure is not quantum mechanically stable due to the non-zero number of negative modes obtained with the RHF/6-31G** method for all values of R . This instability is probably due to the surface effects, and interaction of neighboring clusters in a sufficiently large cluster may reduce this instability.

CONCLUSION

RHF/6-31G** computations carried out in this study showed that 3-D helium clusters have lower electronic energies compared to the isolated helium atoms. The per-atom binding energy and the optimized lattice parameter do not depend significantly on the number of atoms of the cluster. Analysis of the R -dependent properties showed that the 3-D cubic, hexagonal and trigonal clusters of helium are quantum mechanically stable over a relatively wide range of the lattice parameter. This shows that in a thermalized liquid He at high temperatures and in a polycrystalline solid He, many different clusters with different lattice types may exist. More accurate and detailed structural, electronic and thermodynamic analyses would be possible when all computations are carried out at higher levels of theory such as MP2 and MP4 and at low temperatures and high pressures. These calculations are underway in our research group.

Interest in the synthesis and study of materials at nano-scale has been ever increasing since the emergence of nano-science and technology. At this scale, atoms and molecules may form different clusters with different chemical and physical characteristics. This interest is intensified for the case of helium which has the weakest inter-atomic interactions in the liquid and solid phases, and thus a range of sizes and shapes are expected for the assembly of helium atoms in these condensed phases.

Recently, McKellar et al. have been able to produce small clusters ($N < 1000$) of He solvating different species.³¹⁻³² They have used spectroscopic techniques to probe properties of the molecules solvated in these nano-clusters. Results of theoretical studies such as those reported here but obtained at a higher level of theory would serve as a reference for evaluating experimental data such as those reported by McKellar et al.

Application of liquid helium in cryogenic systems increases the importance of such theoretical studies which

can be used to predict its refrigeration behavior from characteristics of the different clusters forming the fluid at the given thermodynamic conditions.³³

Received October 18, 2006.

REFERENCES

- Ng, C. Y.; Baer, T.; Powis (Eds.), I. *Cluster Ions*; Wiley: New York, 1993.
- Kalus, R.; Paidarová, I.; Hrivňák, D.; Paška, P.; Xavier Gadéa, F. *Chem. Phys.* **2003**, *294*, 141-153.
- Chaban, G. M. *Chem. Phys. Lett.* **2005**, *401*, 318-322.
- Castleman, A. W.; Keesee, R. G. *J. Phys. Chem.* **1996**, *100*, 12911.
- Kalcher, J.; Sax, A. F. *Chem. Rev.* **1994**, *94*, 2291.
- Castleman, A. W.; Keesee, R. G. *Chem. Rev.* **1986**, *86*, 589.
- Rucht, T.; Forde, K.; Callicoat, B. E.; Ludwigs, H.; Janda, K. C. *J. Chem. Phys.* **1998**, *109*, 10679.
- See special issue: *J. Chem. Phys.* **2001**, 115 (December 8).
- Yurtsever, E.; Sebastianelli, F.; Gianturco, F. A. *Computational Materials Science* **2006**, *35*, 163-168.
- Cotton, F. A.; Wilkinson, G. *Advanced Inorganic Chemistry*; Wiley: New York, 1999.
- Agrawal, B. K.; Yadav, P. S.; Yadav, R. K.; Agrawal, S. *Prog. Cryst. Growth Charact. Mater.* **2006**, 1-6.
- Manninen, K.; Häkkinen, H.; Manninen, M. *Computational Materials Science* **2006**, *35*, 158-162.
- Häkkinen, H.; Moseler, M. *Computational Materials Science* **2006**, *35*, 332-336.
- Frenking, G.; Cremer, D. *Struct. Bond.* **1990**, *73*, 17.
- Leopold, K. R.; Fraser, G. T.; Novick, S. E.; Klemperer, W. *Chem. Rev.* **1994**, *94*, 1807.
- Bieske, E. J.; Dopfer, O. *Chem. Rev.* **2000**, *100*, 3963.
- Bellert, D.; Breckenridge, W. H. *Chem. Rev.* **2002**, *102*, 1595.
- Liebman, J. F.; Deakyne, C. A. *J. Fluorine Chem.* **2003**, *121*, 1.
- Toennies, J. P.; Vilesov, A. F. *Angew. Chem. Int. Ed.* **2004**, *43*, 2622.
- Lide, D. R. (Ed.) *CRC Handbook of Chemistry and Physics*; 74th ed.; CRC Press: Boca Raton, 1993.
- Grandinetti, F. *Int. J. Mass Spectrom.* **2004**, *237*, 243-267.
- Kent, A. *Experimental Low Temperature Physics*; Macmillan: London, 1993.
- Kittel, C. *Introduction to Solid State Physics*; Wiley Eastern: New York, 1993.
- Sabzyan, H.; Zanjanchi, F. *J. Chin. Chem. Soc.* **2007**, *54*, 303-312.
- Frisch, M. J.; Trucks, G. W.; Schlegel, H. B.; Scuseria, G. E.; Robb, M. A.; Cheeseman, J. R.; Zakrzewski, V. G.; Montgomery, J. A., Jr.; Stratmann, R. E.; Burant, J. C.; Dapprich, S.; Millam, J. M.; Daniels, A. D.; Kudin, K. N.; Strain, M. C.; Farkas, O.; Tomasi, J.; Barone, V.; Cossi, M.; Cammi, R.; Mennucci, B.; Pomelli, C.; Adamo, C.; Clifford, S.; Ochterski, J.; Petersson, G. A.; Ayala, P. Y.; Cui, Q.; Morokuma, K.; Malick, D. K.; Rabuck, A. D.; Raghavachari, K.; Foresman, J. B.; Cioslowski, J.; Ortiz, J. V.; Stefanov, B. B.; Liu, G.; Liashenko, A.; Piskorz, P.; Komaromi, I.; Gomperts, R.; Martin, R. L.; Fox, D. J.; Keith, T.; Al-Laham, M. A.; Peng, C. Y.; Nanayakkara, A.; Gonzalez, C.; Challacombe, M.; Gill, P. M. W.; Johnson, B. G.; Chen, W.; Wong, M. W.; Andres, J. L.; Head-Gordon, M.; Replogle, E. S.; Pople, J. A. *Gaussian 98, A Connected System of Programs for Performing a Variety of Semi-Empirical and Ab Initio Molecular Orbital (MO) Calculations*; Gaussian, Inc.: Pittsburgh, PA, 1998.
- Daunt, J. G.; Edwards, D. O.; Milford, F. G.; Yaqub, M. *Low Temperature Physics Lt19*; Plenum Press: New York, 1965.
- Timmerhaus, K. D.; O'Sullivan, W. J.; Hammel, E. F. *Low Temperature Physics Lt13*; Plenum Press: New York, 1974.
- Donohue, J. *Phys. Rev.* **1959**, *114*, 1009.
- Seyfert, C.; Arms, D. A.; Sinn, H.; Simmons, R. O.; Burkel, E. *Czech. J. Phys.* **1996**, *46*, 471.
- Seyfert, C.; Simmons, R. O.; Sinn, H.; Arms, D. A.; Burkel, E. *J. Phys.: Condens. Matter.* **1999**, *11*, 3501-3511.
- Tang, J.; Xu, Y.; McKellar, A. R. W.; Jäger, W. *Science* **2002**, *297*(5589), 2030-2033.
- Xu, Y.; Jäger, W.; Tang, J.; McKellar, A. R. W. *Phys. Rev. Lett.* **2003**, *91*, 163401.
- Sakurai, A.; Shiotsu, M.; Hata, K.; Takeuchi, Y. *Cryogenics* **1989**, *29*(6), 597-601.